Available online at www.sciencedirect.com
SCIENCE DIRECT®
Journal of Power Sources 138 (2004) 137–144
JOURNAL OF POWER SOURCES
www.elsevier.com/locate/jpowsour

Experimental analysis of water management in a self-humidifying polymer electrolyte fuel cell stack

R. Eckl[a,*], W. Zehtner[a], C. Leu[b], U. Wagner[a]

[a] *Institute for Energy Economy and Application Technology (IfE), Munich University of Technology, Arcisstr. 21, 80333 Munich, Germany*
[b] *Heliocentris Energy Systems GmbH, Rudower Chaussee 29, 12489 Berlin, Germany*

Received 18 September 2003; received in revised form 10 May 2004; accepted 21 June 2004
Available online 13 August 2004

Abstract

The performance of a commercial 300 W_{el} self-humidifying polymer electrolyte fuel cell (PEFC) stack was investigated by studying polarization curves under different operating conditions (temperature, stoichiometry). It could be demonstrated that internal humidification has a major impact on stack performance. Especially when the stack was operated in the low power range at elevated temperatures, dehydration was a serious problem. By applying extreme operating conditions, complete MEA drying-out as well as flooding could be observed. Knowledge of the underlying physical and chemical interrelationships is fundamental for the optimum application and control of polymer electrolyte fuel cell stacks in energy systems.

Keywords: Polymer electrolyte fuel cell stack; Water management; Dehydration; Flooding

1. Introduction

Due to their high efficiency, fuel cells are widely regarded as future power sources. Additional characteristics such as low noise and emission levels as well as excellent scalability open up a magnitude of applications, ranging from power supplies for portable devices to vehicle propulsion systems. Meanwhile, many companies and research institutes worldwide are engaged in developing and commercialising fuel cells. The transition from laboratory scale applications to demonstration plants or small-scale production has already taken place or is about to happen. Fuel cells will gain significant market shares if power density and lifetime will be increased and, at the same time, production costs will be reduced [1].

Within the scope of this communication, a commercially available, self-humidifying fuel cell stack from Heliocentris Energy Systems (Berlin, Germany) with a rated electrical power output of 300 W was analysed. The fuel cell stack is embedded in a demonstration system for combined production of heat and electricity. In the following, the electrical performance characteristics under different operating conditions are presented and special attention is paid to internal water management issues.

2. Water transport in polymer electrolyte fuel cells

In a polymer electrolyte fuel cell (PEFC), hydrogen and oxygen react electrochemically to water, generating electricity and heat. A single PEFC consists of a membrane electrode assembly (MEA) sandwiched between gas diffusion layers and flowfield plates into which gas channels have been machined. The MEA comprises two electrodes, anode and cathode, which are separated by a gas tight, proton conducting membrane (Fig. 1). At the anodic membrane–electrode interface, hydrogen is oxidized electrochemically and

* Corresponding author. Tel.: +49 89 289 23977; fax: +49 89 289 28313.
E-mail address: reckl@ewk.ei.tum.de (R. Eckl).

0378-7753/$ – see front matter © 2004 Elsevier B.V. All rights reserved.
doi:10.1016/j.jpowsour.2004.06.042

Nomenclature

b	Tafel slope (V/dec)
F	Faraday constant (9.6485×10^4 As/mol)
I	load current (A)
M	mass transport overpotential parameter (V)
n	molar flow (mol/s)
N	mass transport overpotential parameter (A^{-1})
p	pressure (bar)
R	ohmic resistance (Ω)
V	voltage (V)
$\dot{V}$	volumetric flow (m^3/s)
x	fraction of gas species (%)

Greek letters

ϑ	temperature (°C)
λ	stoichiometry
φ	relative humidity (%)

Subscripts

air	air on cathode side
critical	critical value
FC	fuel cell stack
H_2	hydrogen on anode side
H_2O	water produced
in	stack inlet
n	single cell index (1 . . . 20)
o	open circuit
O_2	oxygen on cathode side
out	stack outlet
sat	saturation
water	water in airflow

the resulting protons are conducted through the membrane. At the cathodic membrane–electrode interface, oxygen is reduced electrochemically, yielding water as product.

The proton conductivity of the membrane and thus performance of a PEFC decreases rapidly when the water content of the membrane decreases. Especially if the fuel cell is operated with dry reactant gases and product water originating from the electrochemical reaction represents the only source of humidity, an effective water management within the cell is crucial. The amount of water n_{H_2O} produced by the electrochemical reaction in a single cell is directly proportional to the load current I:

$$n_{H_2O} = \frac{I}{2F} \tag{1}$$

This product water is transported along the gas channels as well as in the direction perpendicular to the MEA (Fig. 1). When a current is drawn from the fuel cell protons migrate through the membrane. Depending on the hydration state of the membrane, proton migration is associated with a drag of water molecules from the anode to the cathode side [2,3]. This so-called electro-osmotic transport, together with electrochemical water production, results in an accumulation of water at the cathode side. In turn, the water concentration gradient between anode and cathode causes back diffusion, which works against drying of the membrane from the anode side. The gradient between anodic and cathodic water concentration is determined by the thickness of the membrane, water content of the membrane and humidity of the reactant gases. The latter in turn is dependent on the gas inlet humidification and on the temperature and pressure in the gas channels [4,5].

Maintaining a high water content in the electrolyte is fundamental to ensure high ionic conductivity. Without adequate water management, an imbalance will appear between water production and water removal from the cell. If more water is exhausted than produced and the incoming gases are not humidified, dehydration of the polymer membrane respectively the MEA structure occurs. If there is too much humidity in the cell, however, the electrodes may flood which causes problems with gas diffusion to the electrochemically active layers. Both effects have an adverse impact on

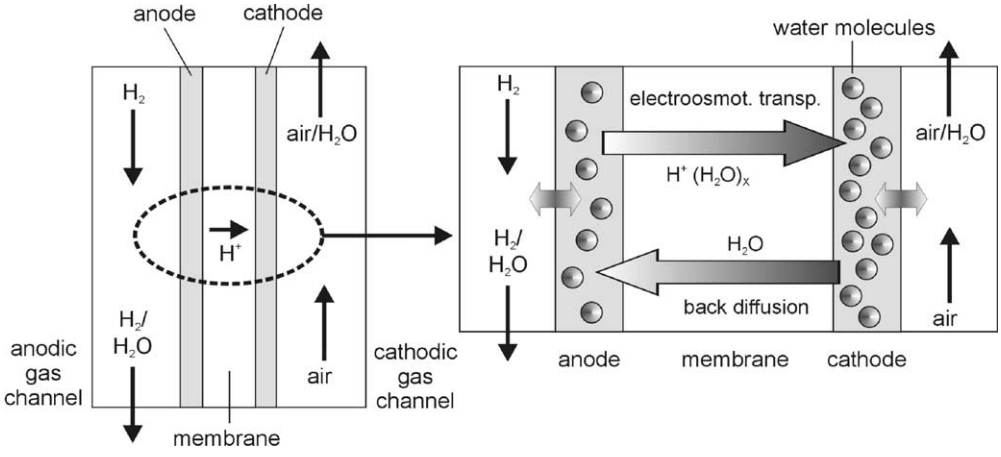

Fig. 1. Water transport in polymer electrolyte fuel cells.

cell performance and can, in the long run, damage the fuel cell.

In a fuel cell stack with series connected single cells, operating conditions may vary significantly not only in the plane of the MEA but also along the stack axis. For example, an even fluid distribution to all the individual cells as well as a homogeneous temperature distribution are difficult to achieve [6]. Due to the fact that these operating parameters directly affect water management, it is an even more challenging task to maintain a proper water balance in a fuel cell stack than in a single cell alone.

3. Equipment description

The computer controlled fuel cell system (Fig. 2) is designed for operation with hydrogen and air. The self-humidifying fuel cell stack consists of 20 water-cooled single cells, each with an active area of 49 cm^2. GORE PRIMEA 5510 MEAs are used with an ionomer thickness of 25 μm and a platinum loading of 0.3 mg/cm^2 on the anode and cathode side, respectively. Gas diffusion layers are GORE CARBEL CL gas diffusion media. The reactant gases and the cooling liquid are fed in parallel to the individual cells of the stack. Hydrogen and air are conducted in cross-flow mode by a two-channel meander on the anode side and a four-channel meander on the cathode side of each single cell.

Ambient air is supplied to the stack by two variable speed diaphragm compressors (KNF Neuberger N 838 KNDC) according to the characteristics given in Fig. 3. Due to strong fluctuations, no reliable airflow rates could be measured for currents below 2 A. The air stoichiometry of λ_{air} = 10 at 2.2 A stack current is rather high; for currents above 20 A, λ_{air} is below 3.2. As an additional option, the airflow can be set manually between 90 and 120% of the automatically adjusted airflow rate from a PC based graphical user interface. Exhaust air is released into the environment via a water separator and a flow restrictor. As there is no pressure control, the air pressure at stack entrance varies between ambient pressure and 1.35 bar_{abs}, depending on airflow.

Hydrogen is fed into the stack in “dead end” mode from a gas bottle via a pressure reducer, main valve and flow meter (OMEGA FMA 3100 series). In order to remove inert gaseous residua and product water originating from back diffusion, a solenoid purge valve is attached to the anodic stack exit. Depending on the load current, the purge valve is periodically activated for about one second by the control programme. All of the experiments were carried out at 1.5 bar_{abs} hydrogen inlet pressure.

Measurement of the individual single cell voltages, stack voltage and temperatures is done by a microcontroller (Atmel Mega103) with analogue and digital input ports. The single cell voltages are fed to the microcontroller via three multiplexer units (MAX307CPI), the stack voltage is measured via a potential divider. Temperatures are measured by digital sensors (Maxim-Dallas DS1820) via an interface IC and a one-wire bus.

The electric current generated by the fuel cell stack is sunk by an electronic load box (zentro-elektrik ELA 500/20/50-1), which provides a current-proportional 0–5 V signal to the microprocessor unit. For stack cooling, distilled water is pumped in a closed circuit with a cooler and a variable

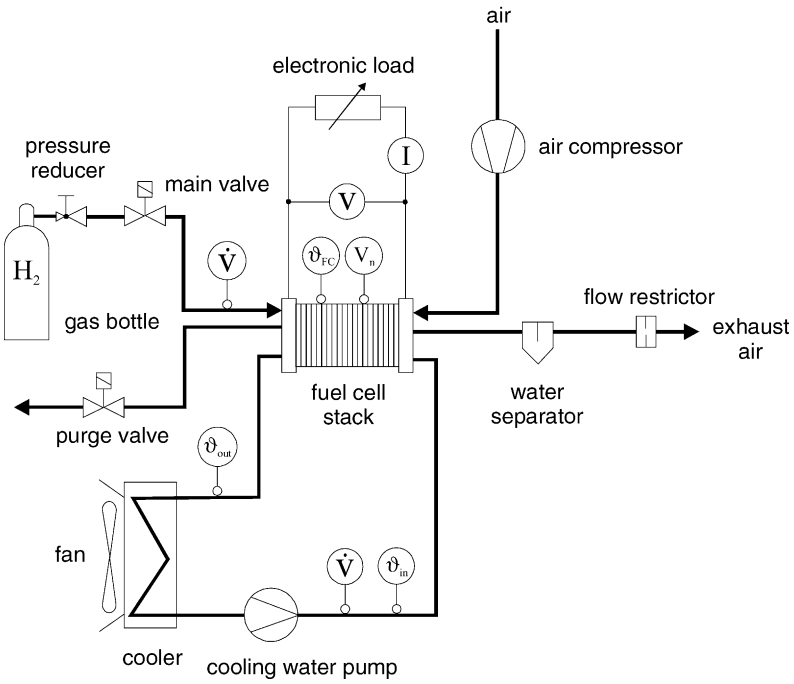

Fig. 2. Heliocentris fuel cell system layout.

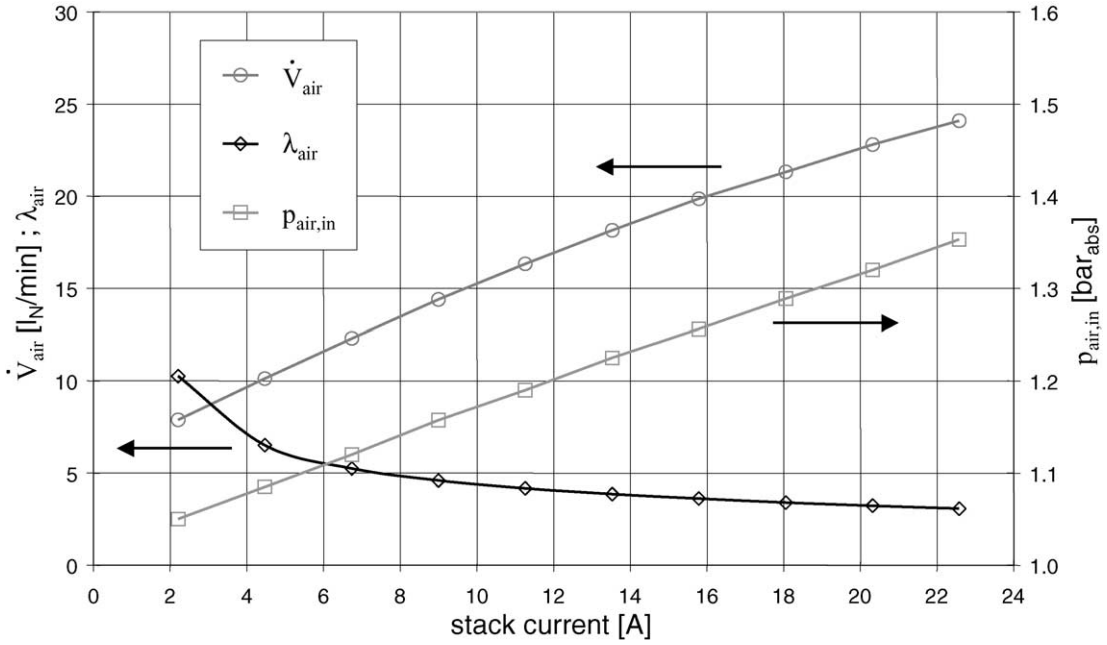

Fig. 3. Airflow, air stoichiometry and air pressure at stack entrance against load current.

speed fan. The PC control programme is continuously monitoring the operating parameters and shuts down the system if a single cell voltage drops below 400 mV or if stack temperature rises above 70 °C. If the load is too high and the stack terminal voltage drops below 12 V, the load current is reduced automatically.

4. Polarization curves at different operating temperatures

In general, the performance of PEFCs shows a strong dependence on operating temperature. The reversible potential decreases with increasing temperature, but performance actually increases because of an increase in reaction rate and a higher mass transfer rate. With an increase in operating temperature, however, a higher rate of evaporation occurs and the reactant gases can take up more water vapour because of higher saturation pressure. Without reliable forms of water management, the MEA structure may start to dry out, resulting in lower ionic conductivity and higher charge transfer resistance across the electrode–electrolyte interface [5,7,8].

In order to evaluate the influence of temperature on the performance of the 300 W_{el} PEFC stack, the polarization curves depicted in Fig. 4 were recorded. The experiments started at

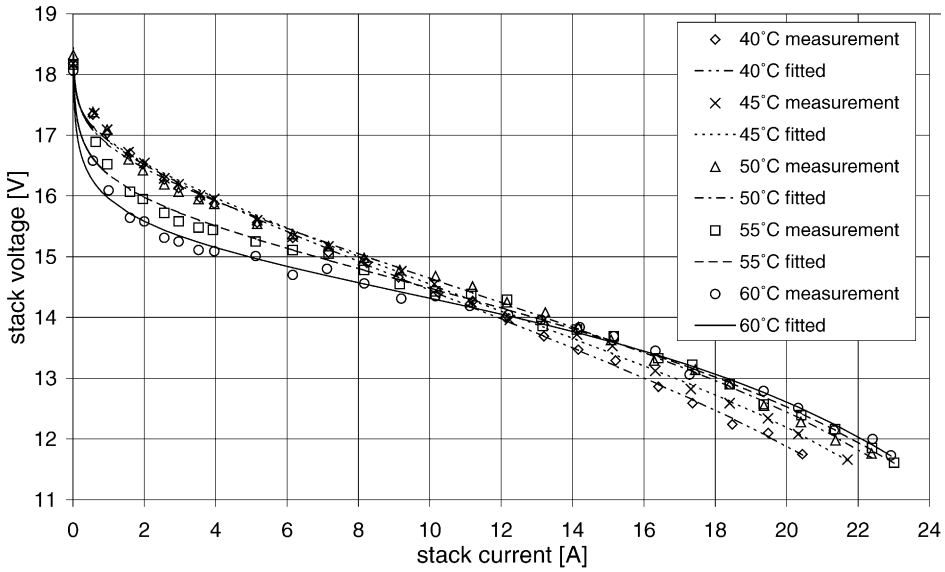

Fig. 4. Polarization curves at different operating temperatures (points are measured values, lines represent interpolations according to Eq. (2)).

the highest possible stack currents, followed by a successive current reduction in 1 A steps. Due to the fact that polarization curves show a particularly non-linear characteristic at high loads, the current steps were reduced to 0.5 A for stack currents below 4 A. Each operating point was maintained for about 40 s and after data acquisition the purge valve was activated manually. The comparatively high scan rate of 40 s per operating point was chosen to avoid membrane drying-out at low stack currents and high air stoichiometries (Fig. 3), though it prevents the stack from reaching equilibrium conditions during the experiments. The problem of drying-out will be discussed in detail below.

The stack voltages depicted as points in Fig. 4 can be described mathematically by evaluating the parameters V_o, b, R, M and N of the equation [9]

$$V = V_o - b \times \log I - R \times I - M \times \exp(N \times I) \quad (2)$$

In this equation, V_o represents the open circuit voltage, b is the Tafel slope, R is the ohmic resistance, and M and N are parameters accounting for the mass transport overpotential. The respective data sets were fitted with Eq. (2) and the resulting polarization curves are depicted as lines in Fig. 4.

It is obvious from Fig. 4 that the polarization curves do show significant temperature dependence. As all curves intersect in the medium current region, it is not possible to specify an optimal operating temperature for the entire load range. For load currents below 12 A, the stack shows best performance at 40–50 °C operating temperature. At 55 and 60 °C, a strong activation overpotential component can be observed. This indicates dehydration, which adversely affects the resistance of the ionomeric component within the catalyst layer and increases the interfacial charge transfer resistance, i.e. higher losses in the activation energy occur [5,8,10,11].

According to [4], operation with dry gases is possible if the amount of product water is sufficient to saturate the outlet gases, respectively if the following criterion is satisfied:

$$1 \geq \left(\lambda_{H_2} - 1 + \frac{\lambda_{air}}{2x_{O_2}} - \frac{1}{2}\right) \times \frac{p_{sat}(\vartheta_{FC})}{p - p_{sat}(\vartheta_{FC})} \quad (3)$$

where λ_{H_2} represents the hydrogen stoichiometry, x_{O_2} is the fraction of oxygen in the airflow (20%), p is the total pressure in bar_{abs} (by approximation $p_{air,in}$ from Fig. 2) and p_{sat} is the saturation pressure of water vapour, depending on air temperature ϑ_{air} (by approximation ϑ_{FC}). For dead-end operation at the hydrogen side ($\lambda_{H_2} = 1$), a critical air stoichiometry for internal humidification can be derived from Eq. (3):

$$\lambda_{critical} = 0.2\left(\frac{2p}{p_{sat}(\vartheta_{FC})} - 1\right) \quad (4)$$

As pressure varies with airflow in our application, $\lambda_{critical}$ is not only a function of saturation pressure and thus operating temperature but also of stack current. In Fig. 5, λ_{air} and $\lambda_{critical}$ at different operating temperatures are depicted against stack current.

It can be noted from Fig. 5 that λ_{air} exceeds the critical value independently of operating temperature for stack currents below 5 A. At operating temperatures below 50 °C, saturation of the airflow is possible if the stack currents are greater than those defined by the intersections of the air stoichiometry curve with the respective critical curves. At 55 °C, the criterion given by Eq. (3) is just about satisfied for stack currents above 20 A. At 60 °C, the air stoichiometry is only approaching the critical values at very high stack currents.

From these results it can be concluded that the high activation polarisation at 55 and 60 °C operating temperature is in fact caused by strong dehydration of the MEAs during the course of the experiments. At lower operating temperatures, internal humidification of the airflow is possible over a more or less expanded current range. Consequently, dehydration sets in later and activation polarisation is less pronounced

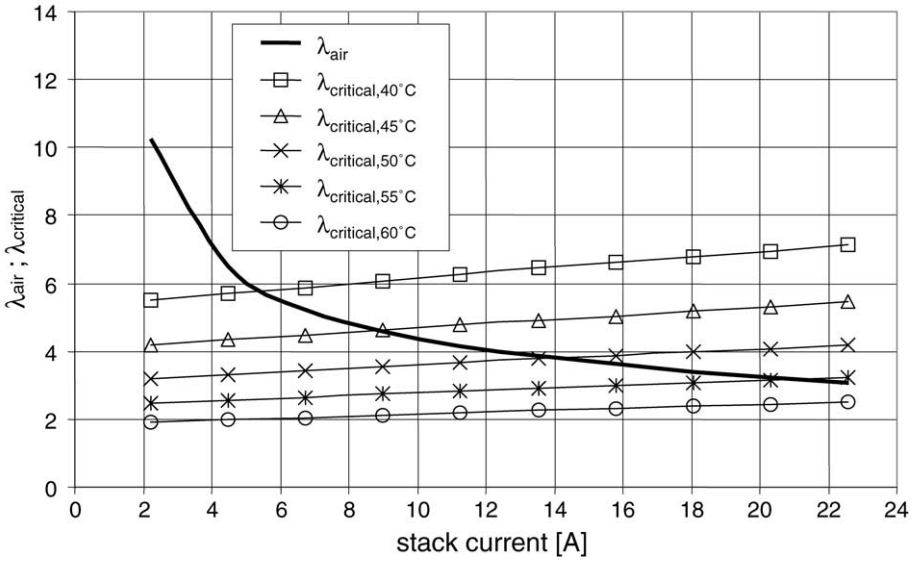

Fig. 5. Air stoichiometry and critical stoichiometries against stack current.

towards the end of the low temperature experiments. However, drying-out of the membrane will always occur below a certain stack current, which explains the necessity for the relatively high scan rate.

For the interpretation of the stack behaviour at high currents (16 A and above), the sharp criteria given by Eqs. (3) and (4) need to be relativised to some extent. In practice, ambient air is fed into the fuel cell stack with a relative humidity greater than zero as assumed above. More important, not the complete amount of product water is evaporated to humidify the airflow through the stack. The actual relative humidity of the exhaust air is equal to

$$\varphi_{\text{air}} = \frac{p}{p_{\text{sat}}(\vartheta_{\text{FC}}) \times (1 + n_{\text{air}}/n_{\text{water}})} \quad (5)$$

where n_{air} represents the molar airflow through the stack and n_{water} is the amount of water contained therein. By measuring the water condensation rate in the water separator at different operating points and applying these values for n_{water} in Eq. (5), the outlet humidity could be estimated. It turned out that φ_{air} was considerably lower than theoretically possible, i.e. when the complete amount of product water would have been evaporated. Additionally, liquid water was exhausted from the anode side when the hydrogen purge valve was activated even at medium currents and high temperatures (e.g. I = 10 A and $\vartheta_{\text{FC}} = 60\,^{\circ}\text{C}$). This indicates back diffusion and water accumulation at the anode side, which in turn prevents the MEA from drying-out and allows for stable operation of the stack.

From these observations, we may assume that MEA dehydration is actually not a problem at elevated temperatures when water production is sufficiently high and air stoichiometries are less excessive, i.e. when the stack is operated at medium to high currents (Eq. (1)) and the differences between λ_{air} and $\lambda_{\text{critical}}$ are less pronounced (Fig. 5). Local dehydration cannot be excluded but favourable effects associated with elevated operating temperature (increased reaction rates, higher mass transfer rates) result in better overall performance. The maximum power output at 60 °C operating temperature is 269 W compared to 240 W at 40 °C, which represents a performance gain of 12%. However, for the big differences between λ_{air} and $\lambda_{\text{critical}}$, the above considerations concerning dehydration remain valid.

5. Drying-out and flooding of the PEFC stack

The above experiments clearly demonstrated the fundamental effect of water management on stack performance. In the following, drying-out and flooding at extreme operating conditions will be investigated.

For MEA drying-out, water removal from the stack must be higher than water production. Little water production is equivalent to small load currents, high water removal is achieved by elevated air stoichiometries and temperatures. Preconditioning of the stack was done at 10 A load current and 50 °C operating temperature for about 20 min, i.e. we can assume well-humidified initial conditions from the observations in the previous section.

The experiment depicted in Fig. 6 started with stack temperature ϑ_{FC} = 49 °C, air stoichiometry λ_{air} = 6 and stack current I = 5 A. To facilitate the observation of differences in single cell voltages, the current was shortly increased to 10 A every 5–8 min. In Fig. 6, stack temperature, stack current and

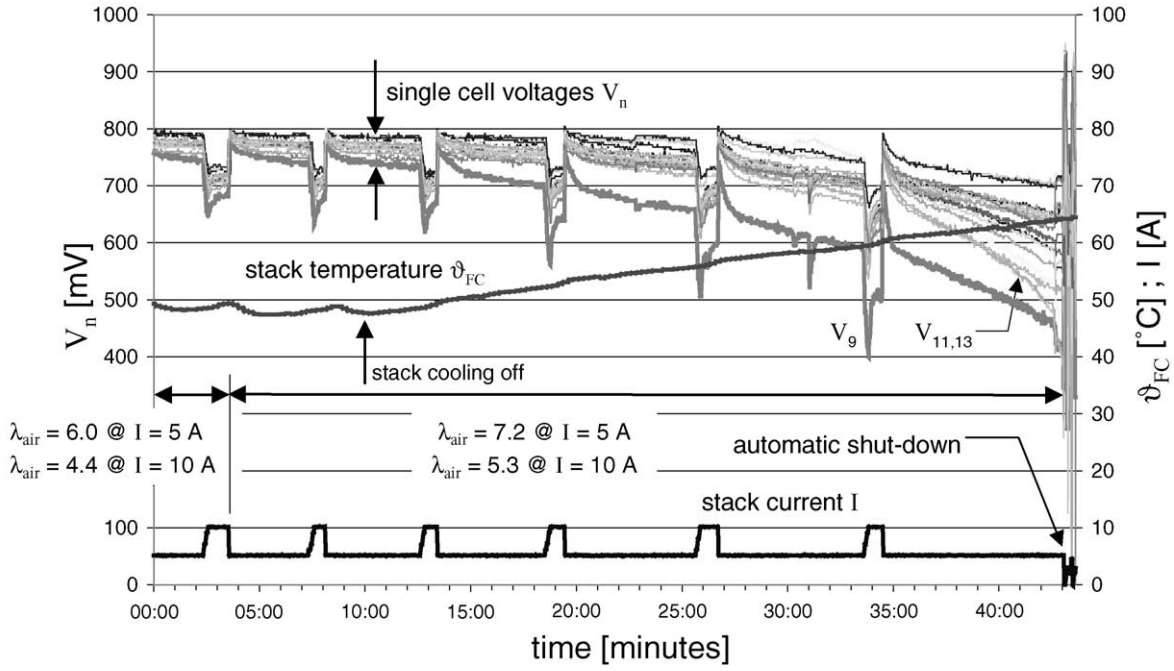

Fig. 6. Drying-out of the fuel cell stack.

the 20 single cell voltages are recorded. To accelerate MEA dehydration, the airflow was increased to λ_{air} = 7.2 after the first load step. To further enforce drying-out, stack cooling was switched off 10 min after the beginning of the experiment. As a consequence, ϑ_{FC} increased to approximately 65 °C.

Due to MEA dehydration, the single cell voltages were decreasing during the experiment. The control programme shut down the system after 43 min because several single cell voltages (V_9, V_{11}, V_{13}) dropped below the critical threshold of 400 mV. It can be noted from Fig. 6 that the individual cells of the stack were not equally affected by dehydration and that the differences became more pronounced with increasing length of time. Cells numbers 9, 11 and 13, which are located close to the centre of the stack, revealed the worst performance. This is presumably due to more pronounced dehydration as a consequence of a non-uniform temperature field with local overheating in the central domain.

During the load steps from 5 to 10 A, a voltage drop could be observed for each single cell, followed by a distinct phase of regeneration. This regeneration continued to have a short-term positive effect on cell performance after taking back the stack current to 5 A again. Obviously, increased water production and a reduced air stoichiometry of λ_{air} = 5.3 during periods with 10 A load current at least partially compensated dehydration and thus temporarily reduced the overpotentials.

For stack flooding, the procedure for drying-out was inverted. Preconditioning of the stack was done at 10 A load current and 40 °C operating temperature for about 20 min, i.e. we can assume rather humid starting conditions (Fig. 5). In order to achieve a compromise between high water production and as low as possible heat generation for the experiment, the load current was maintained at 10 A, which was associated with an air stoichiometry of 4.4. To minimize water evaporation, stack cooling was set to maximum performance, resulting in a stack temperature slightly below 40 °C. After 3 min, λ_{air} was reduced manually to 4.0. In Fig. 7, stack temperature, stack current and the 20 single cell voltages are depicted.

During the complete course of the experiment, various single cells show regular voltage drops, especially cell numbers 3 and 5. It can be assumed from Fig. 5 that well-humidified operation of the stack is guaranteed at 10 A load current and reduced air stoichiometry. However, excess water becomes a problem when it prevents gaseous reactants from reaching the electrochemically active layers. Each time the purge valve was activated, a significant amount of liquid water was exhausted from the stack. At the same time, an instantaneous regeneration of the individual single cells showing reduced voltage performance could be observed (Fig. 7). This leads to the conclusion that water originating from back diffusion caused MEA flooding at the anode side. Furthermore, it cannot be excluded that liquid water accumulated in the gas channels and thus prevented a homogeneous reactant distribution across the active area. As soon as an individual single cell voltage dropped below 400 mV, the purge valve was opened automatically and prevented system shutdown if the voltage jumped up immediately. This was the case for cell number 3 after about 16 min and cell number 5 after about 18 min. After 19 min, the stack current was increased to 12 A, resulting in shorter purging cycles due to potential drops below 400 mV of cell number 5. When the stack current was further increased to 14 A, V_5 dropped below 400 mV and did not regenerate despite immediate purging. Due to advanced

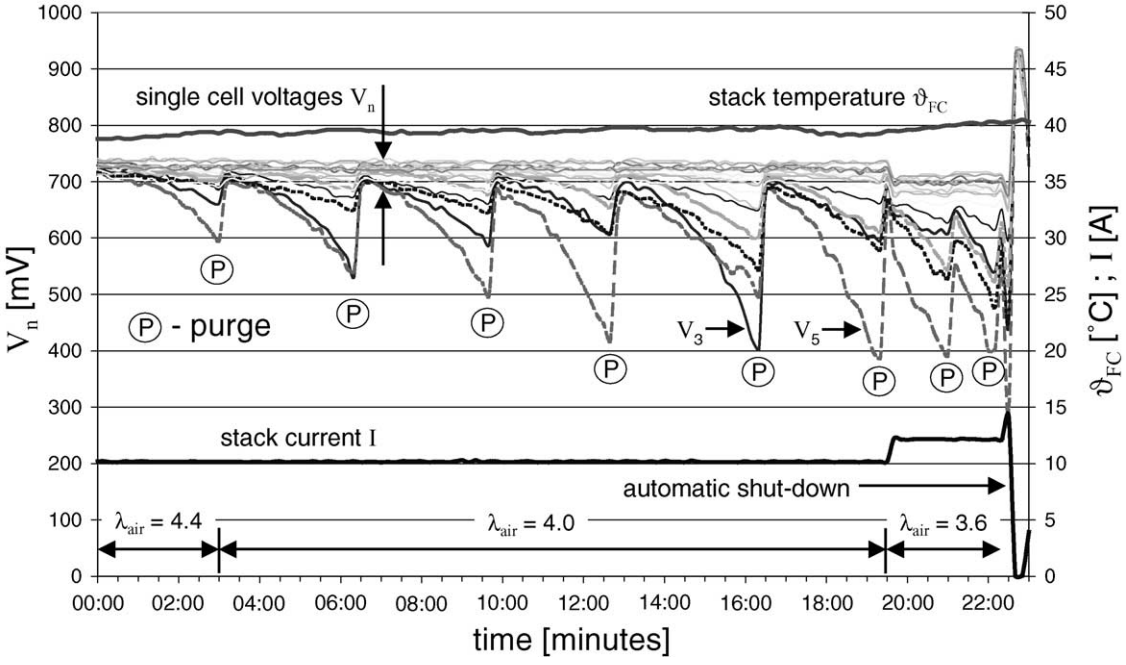

Fig. 7. Flooding of the fuel cell stack.

MEA flooding, not enough water could be removed from the anode side to maintain a load current of 14 A. Consequently, the control programme shut down the system.

6. Conclusions

By investigating the electrical performance characteristics of a 300 W_{el} PEFC stack under different operating conditions, it could be demonstrated that water management is of prime relevance. Self-humidifying operation of the stack as well as optimisation of electrical power output is possible, if excessive dryness or humidity is prevented by carefully adjusting the operating conditions. Even though the control programme allows for setting the operating parameters only within a relatively narrow range, complete MEA drying-out and flooding is possible. As the PEFC stack itself forms a complex system with a magnitude of interactions, each operating parameter must be considered in a systematic context.

At low currents, the PEFC stack is fed with ambient air at rather high stoichiometries. Consequently, drying-out is a serious danger if the stack is operated in the low power region for a longer period. According to the manufacturer, stack performance was optimised near the maximum power point for a first approach and the respective compressor speeds were evaluated empirically. In future system respectively software generations, the airflow will be set to lower stoichiometries in the lower power range as well. The performance data presented in this communication including the derivation of critical stoichiometries are well suitable to yield reference values for reengineering the control programme.

Acknowledgments

The authors wish to thank Dr. W. Lehnert, Centre for Solar Energy and Hydrogen Research (Ulm, Germany), for valuable suggestions.

References

[1] M.L. Perry, T.F. Fuller, J. Electrochem. Soc. 149 (2002) S59–S67.
[2] T.A. Zawodzinski, J. Davey, J. Valerio, S. Gottesfeld, Electrochim. Acta 40 (1995) 297–302.
[3] T.A. Zawodzinski, T.E. Springer, J. Davey, R. Jestel, C. Lopez, J. Valerio, S. Gottesfeld, J. Electrochem. Soc. 140 (1993) 1981–1985.
[4] G.J.M. Janssen, M.L.J. Overvelde, J. Power Sources 101 (2001) 117–125.
[5] J.H. Hirschenhofer, D.B. Stauffer, R.R. Engleman, M.G. Klett, Fuel Cell Handbook, fourth ed., U.S. Department of Energy, Office of Fossil Energy, Federal Energy Technology Center, 1998.
[6] P. Rodatz, F. Büchi, C. Onder, L. Guzzella, J. Power Sources 128 (2004) 208–217.
[7] S.O. Morner, S.A. Klein, J. Solar Energy Eng. 123 (2001) 225–231.
[8] F. Liu, B. Yi, D. Xing, J. Yu, Z. Hou, Y. Fu, J. Power Sources 124 (2003) 81–89.
[9] J. Kim, S.M. Lee, S. Srinivasan, C.E. Chamberlin, J. Electrochem. Soc. 142 (1995) 2670–2674.
[10] T.E. Springer, T.A. Zawodzinski, M.S. Wilson, S. Gottesfeld, J. Electrochem. Soc. 143 (1996) 587–599.
[11] G.J.M. Jansen, J. Electrochem. Soc. 148 (2001) A1313–A1323.